

and to thank Dr. M. C. Michel and Dr. F. A. Asaro for their help with several of the experiments.

## APPENDIX

### Calibration of the NaI(Tl) Spectrometer

A  $1\frac{1}{2}$ -inch diameter by 1-inch thick thallium activated sodium iodide crystal was used in conjunction with the 50-channel analyzer. A diffuse reflector of MgO surrounded the crystal, and a thin beryllium window separated it from the sample. The crystal was bonded to a thin quartz disk which in turn was optically coupled to a Dumont 6292 photomultiplier tube by a layer of mineral oil. With this arrangement, a resolution of 8 percent was obtained at 661 kev. An aluminum-lined lead shield housed the detector assembly, and samples were mounted in a standard G-M tube five position shelf holder. In these experiments, most measurements were made at a distance of  $\sim 1.5$  inches from the crystal, which represented a geometry of 5.1 percent (as determined with the 60-kev gamma ray of a standardized Am<sup>241</sup> sample).

Energy calibration of the spectrometer was made during each experiment, with the following gamma-ray standards: Am<sup>241</sup> (60 kev), U<sup>235</sup> (143, 184 kev), Au<sup>198</sup> (412 kev), Cs<sup>137</sup> (32, 661 kev), and Na<sup>22</sup> (510 kev, 1.28 Mev). In addition, the annihilation radiation of Cs<sup>126</sup>

served as an internal standard, so that any shift in the energy scale could be observed and corrected.

The following counting efficiencies were used to calculate the relative intensities of the various gamma rays:

X-rays (Cs, Xe)	100 percent
225 kev	63
385 kev	28
510 kev	17
700 kev	11

We have determined the counting efficiencies of gamma rays at 412 kev (Au<sup>198</sup>), 510 kev (Na<sup>22</sup>), 661 kev (Cs<sup>137</sup>), 1.28 Mev (Na<sup>22</sup>), and 1.33 Mev (Co<sup>60</sup>), using a  $4\pi$  counter to determine the absolute disintegration rates of the standard samples. The results of these measurements were all within 5 percent of the efficiencies obtained from the data of Bell *et al.*<sup>17,18</sup> for the experimental conditions used here. Because of this agreement, the Oak Ridge curves were used to determine the efficiencies at other gamma-ray energies.

The observed x-ray intensities were corrected for fluorescence yield and absorption by comparison with the x-rays from a Cs<sup>137</sup> standard examined under identical experimental conditions.

<sup>17</sup> Bell, Heath, and Davis, Oak Ridge National Laboratory Report ORNL-1415, 1952 (unpublished).

<sup>18</sup> Bell, Hughes, Davis, Jordan, and Randall, Oak Ridge National Laboratory Report ORNL-1415, 1952 (unpublished).

## Neutral Pion-Deuteron Production in 400-Mev $n$ - $p$ Collisions\*

R. A. SCHLUTER

*Institute for Nuclear Studies, The University of Chicago, Chicago, Illinois*

(Received June 17, 1954)

The reaction  $n + p \rightarrow d + \pi^0$  has been studied in a high-pressure hydrogen-filled diffusion cloud chamber. A total of 102 deuterons were identified by a technique of ionization measurement in conjunction with momentum measured in the 10 500-gauss magnetic field. From the laboratory deuteron angle and momentum, the pion angle and the incident neutron energy can be deduced with good resolution, provided the pion is emitted backward in the center-of-mass system. Proton recoils were observed simultaneously, from which the incident neutron flux and energy spectrum were determined. The energy spectrum is centered at 400 Mev with a spread of  $\pm 25$  Mev. From 52 events occurring in the backward direction the angular distribution of pion emission was found to be consistent with  $(0.28_{-0.14}^{+0.26} + \cos^2 \bar{\psi}_\pi)$ , where the

limits include 70 percent of the probability and  $\bar{\psi}_\pi$  is the pion angle in the center-of-mass system. The observed excitation function and total cross section determined from 60 events is consistent with  $(0.47 \pm 0.08)\eta^3$  millibarn, where  $\eta$  is the center-of-mass pion momentum in rest mass units. These results agree, within the accuracy of the measurements, with the prediction of charge independence that the ratio of this reaction to  $p + p \rightarrow d + \pi^+$  should be  $\frac{1}{2}$ .

Eight cases of internal conversion of the neutral pion were seen, four accompanied by deuterons and four by protons, the later giving evidence on neutral pion creation with unbound final nucleons.

## I. INTRODUCTION

THE experiment reported here is a study of the reaction  $n + p \rightarrow d + \pi^0$  in a high-pressure diffusion cloud chamber, with  $400 \pm 25$ -Mev neutrons produced by the University of Chicago 170-inch synchrocyclotron.

\* Research supported by a joint program of the U. S. Office of Naval Research and the U. S. Atomic Energy Commission.

The total cross section as well as the angular distribution were measured. Since deuterons rather than neutral pions were detected, there is in this experiment no ambiguity due to the presence of pions produced with unbound final nucleons. The general plan of the experiment is this: deuterons produced in collisions of 400-Mev neutrons with protons in a high-pressure hydrogen

diffusion cloud chamber were identified by a technique of ionization measurement combined with momentum measurement. From deuteron angle and momentum, and knowledge of the incident beam direction, the pion angle in the center-of-mass system and the incident neutron energy in the laboratory system were deduced for each event. Proton recoils in the forward direction were used to determine the incident neutron flux and energy spectrum.

The principal theoretical interest in this reaction arises from the hypothesis of approximate charge independence in the pion-nucleon interaction. The principle of charge independence reduces to three the number of independent matrix elements required to describe single pion production in nucleon-nucleon collisions. This simplification, together with a phenomenological description of the nucleon-nucleon force, provides a framework in which a consistent explanation of the gross features of these processes, such as meson energy spectrum and variation of yield with incident energy, has been attained,<sup>1</sup> and the success of this scheme is support for the charge independence hypothesis.

An acute further test is afforded by the experimental check of relations predicted by charge independence to exist among the various pion creation cross sections. The simplest of these relations,

$$\sigma(n+p \rightarrow d+\pi^0) = \frac{1}{2}\sigma(p+p \rightarrow d+\pi^+), \quad (1)$$

is found for reactions in which the final nucleons are bound deuterons, because the deuteron has isotopic spin 0 whereas an unbound neutron and proton can have isotopic spin 1 or 0. Under charge independence the two reactions of Eq. (1) are merely different orientations in isotopic spin space of a state of total isotopic spin 1, the factor  $\frac{1}{2}$  coming from the fact that only half of the  $n+p$  states have isotopic spin 1. The similarity of angular distributions predicted by Eq. (1) has been previously confirmed. The angular distribution for  $n+p \rightarrow d+\pi^0$  was measured by Hildebrand;<sup>2</sup> that for  $p+p \rightarrow d+\pi^+$  was obtained by detailed balance from the reaction  $d+\pi^+ \rightarrow p+p$ , which was measured by Durbin, Loar, and Steinberger.<sup>3</sup>

At the energy of this experiment (pions produced with an energy of about 50 Mev in the center-of-mass system) the important final states and corresponding

TABLE I. Final states and corresponding initial states in  $n+p \rightarrow d+\pi^0$ .

	Initial	Deuteron	Pion	$J$	Parity	Ang. dist.
(a)	$^3P_1$	$^3S_1$	$S$	1	-	isotropic
(b)	$^1S_0$	$^3S_1$	$P$	0	+	isotropic
(c)	$^1D_2$	$^3S_1$	$P$	2	+	$\frac{1}{3} + \cos^2$

<sup>1</sup> K. M. Watson and K. A. Brueckner, Phys. Rev. **83**, 1 (1951); M. Gell-Mann and K. M. Watson, Ann. Rev. Nuc. Sci. (to be published); A. H. Rosenfeld, Phys. Rev. **96**, 130, 139 (1954).

<sup>2</sup> R. H. Hildebrand, Phys. Rev. **89**, 1090 (1953), and private communication.

<sup>3</sup> Durbin, Loar, and Steinberger, Phys. Rev. **84**, 581 (1951).

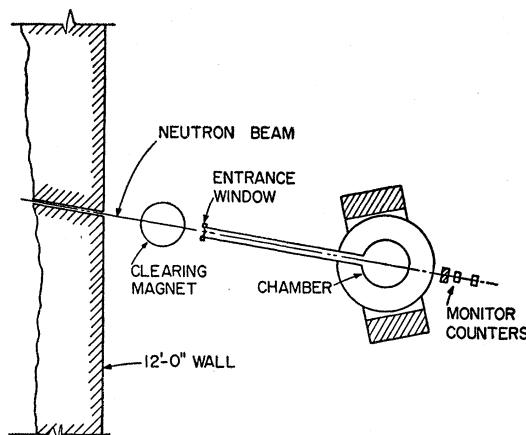


FIG. 1. Experimental arrangement.

initial states allowed by conservation of parity, angular momentum, and isotopic spin for the reaction  $n+p \rightarrow d+\pi^0$  are given in Table I. The angular distributions are for unmixed transitions. The total angular distribution must be symmetric about  $90^\circ$  in the center-of-mass system, because the initial states are symmetric with respect to isotopic spin and the initial nucleons are therefore indistinguishable. There is evidence from pion scattering experiments<sup>4</sup> that the pion-nucleon interaction is strong in two-particle states of spin  $\frac{3}{2}$  and isotopic spin  $\frac{3}{2}$ . Such states are components only of final state (c), so we expect that this transition will be strong<sup>5</sup> and that there will be (1) a prominent  $\cos^2\psi$  term in the angular distribution and (2) a predominantly  $\eta^3$  dependence of the cross section, where  $\eta$  is the center-of-mass momentum in rest-mass units. This has been experimentally confirmed for the analog reaction  $p+p \rightarrow d+\pi^+$ .

## II. EXPERIMENTAL ARRANGEMENT

The general experimental arrangement is shown in Fig. 1. The neutrons were produced in a 2-inch thick beryllium target placed in the circulating proton beam at radius 76 inches, corresponding to a nominal proton energy of 450 Mev. Neutrons emitted directly forward pass through 1-inch collimators at either side of the 12-foot steel shield wall. The angular divergence of the neutron beam was about  $0.2^\circ$ . Near the cyclotron side, an 11-inch long paraffin plug was inserted into the beam under conditions such that a single neutron scattering would almost certainly remove the neutron from the beam. The purpose of this filter was to suppress neutrons of energies less than about 100 Mev. Neutrons of such energies are particularly injurious to diffusion cloud-chamber operation because they produce highly ionizing recoil protons copiously, and these deplete the

<sup>4</sup> Anderson, Fermi, Martin, and Nagle, Phys. Rev. **91**, 155 (1953).

<sup>5</sup> K. A. Brueckner and K. M. Watson, Phys. Rev. **86**, 923 (1952).

vapor supply. At the exit of the collimator a magnet was placed to deflect charged particles away from the chamber. The entrance window for the high-pressure chamber is  $\frac{1}{32}$ -inch stainless steel, and in the neutron beam is a source of charged secondaries which steal vapor and confuse pictures. It was therefore mounted on the end of a  $5\frac{1}{2}$ -foot tube in order to remove it from the vicinity of the sensitive volume of the chamber.

For maintaining the neutron beam intensity at a delicate compromise between chamber overloading and empty pictures, a monitor consisting of an hydrogenous target followed by counters was placed in the neutron beam leaving the chamber. This monitor played no role in measurement of cross section. As a further check on cloud-chamber operation as well as on neutron beam intensity, a small auxiliary camera was mounted to provide test pictures at frequent times during the run without interrupting operation or disturbing the main camera. This camera viewed the heart of the sensitive volume and permitted continual photographic check on cloud-chamber operation.

The chamber itself operated at a pressure (when cold) of 22 atmospheres. It has an inside diameter of 18 inches and maintains a sensitive depth of 2 inches to 3 inches. It is provided with a nonpulsed magnetic field of 10 500 gauss. A proton resonance device was built for measuring the field at several positions in the chamber, and a flux meter using a coil and electronic integrator used to map intermediate regions. The magnetic field varies by one percent across the useful diameter of the chamber, and by about 0.5 percent per cm in the vertical direction in the sensitive volume. Corrections have been made for these variations, although error in radius of curvature measurement usually dominates, as discussed in Sec. III.

The chamber was photographed by a stereoscopic camera whose eyes converge at a total angle of  $16^\circ$ . The camera uses 35-mm Eastman Kodak Linagraph Ortho film, and Leitz Hektor 28-mm lenses which give a minification of 18. Photography is synchronized with the cyclotron oscillator high-voltage power source so that the flash occurs 114 milliseconds after the particles arrive. The clearing field of about 80 volts/cm is removed about four seconds before tracks are formed and reapplied immediately after photography. The interval between exposures was 27 seconds, somewhat longer than in usual diffusion cloud-chamber operation, in order that the chamber could recover fully between pulses. Full recovery and a minimum of localized regions of vapor depletion in the sensitive volume were necessary in order to obtain clear origins of charged recoils. This requirement, plus the fact that the tracks dealt with were relatively heavily ionizing, necessitated the precautions already mentioned, i.e., low-energy neutron filter in the beam, distant chamber entrance window, relatively long interval between pictures, and the auxiliary camera. In addition, great care was taken in shielding of the experimental room and the removal of

weakly radioactive objects from the vicinity of the chamber during the runs.

### III. SCANNING PROCEDURE

The pictures were analyzed by projection through the identical optical system used in photography in order to eliminate distortion of optical origin. Replicas of the plate glass cloud chamber windows were mounted before the lenses. Film shrinkage is negligible provided the time between photography and projection is not more than a few months.

The projection system was designed to allow accurate and rapid angle and momentum measurement. Over 10 000 pictures were scanned and several thousand tracks measured at an over-all rate of about one picture per minute.

The tracks were projected onto a table which tilts about an axis (the  $\phi$  axis) fixed perpendicular both to the direction of the incident beam and to the projection axis. The  $\phi$  axis can be translated horizontally and vertically in order that the origin of a track may be brought into coincidence at a point on the  $\phi$  axis. See Fig. 2. On the table is a protractor to measure the angle in the plane of the table. The table is adjusted so that  $\phi=0$ ,  $\theta=0$  is the direction of the incident beam to within the accuracy of alignment of the cloud chamber, which is to within a few tenths of a degree. This alignment was checked by study of the process  $n+p \rightarrow p+p+\pi^-$ .<sup>6</sup> All final particles are charged, and the resultant momentum direction, which is that of the incident neutron, can be determined. The full angular spread of the neutron beam is  $0.2^\circ$ .

The film was adjusted in the projector by means of three fiducial markers located at the bottom of the chamber. The images of these markers were adjusted by film motion to obtain stereoscopic coincidence at the proper height of the table.

The momentum of a particle was obtained by measuring the radius of curvature in the plane of the table by means of a set of thin plastic sheets scribed with radii in steps of 2.5 cm. The radii measured in this experiment were in the range 180 to 330 cm and were usually measured to the nearest step of 2.5 cm, thereby

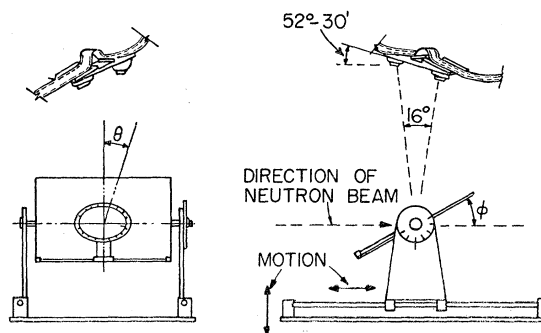


FIG. 2. Essential geometrical features of the scanning projector.

<sup>6</sup> S. C. Wright and R. A. Schluter, Phys. Rev. **95**, 639 (1954).

giving an accuracy in momentum of about one percent. This is the greatest contribution to error in momentum measurement. Superposition of these curves on the track images makes discernible any single Coulomb scatterings of a few tenths of a degree or more. Such scatterings might otherwise lead to error in momentum measurement.

The momentum  $P$  in Mev/ $c$  is given by

$$P = \frac{H_0 \rho'}{3333} \cos \phi \left( 1 - \frac{\theta^2}{4} \right)$$

to second order in  $\theta$ , where  $\rho'$  is the radius measured in the plane of the table,  $H_0$  is the vertical magnetic field in gauss, and the correction term arises from the fact that although the track is a section of a helix, the table is not, in general, exactly in the osculating plane of the helix. For  $\theta \approx \frac{1}{10}$  the correction is 0.2 percent.

The magnetic field is nearly constant throughout the usable chamber volume. Correction for its variation in the vertical direction has been made in deuteron measurement.

#### IV. DETECTION OF DEUTERONS

Deuterons were distinguished from recoil protons by momentum and by a method of ionization measurement. The method and its empirical justification are described, followed by a discussion of factors affecting track image width, and a summary of conditions which it is believed must prevail in order that consistent ionization measurements can be made.

Direct ionization measurement in a high-pressure diffusion cloud chamber must rely on gross features of track appearance, such as width, because counting of individual droplets is not feasible. For example, in hydrogen at 25 atmospheres pressure and 220°K a minimum-ionizing particle produces about 200 ion pairs per cm, a 400-Mev proton twice this.<sup>7</sup> These densities are far too large for usual photographic resolution. Furthermore, densely packed droplets coalesce, so that the number of individual droplets is not simply related to the number of ions. In a diffusion cloud-chamber supersaturation is always present so that ions cannot be dispersed by delaying the onset of drop growth.

In this experiment pictures were scanned in a unit magnification projector as described in Sec. III. The tracks are nearly normal to the projection axis. A simple width-measuring device, two intersecting lines scribed on thin transparent plastic [Fig. 3(a)], was superposed on the track image and adjusted by means of a low-power magnifier so that the skew lines enclose an interval of three times the apparent track width. This criterion avoids obscuring the track edge by the lines, as would occur if the device were adjusted to exactly track width. The widths range from 0.3 to 0.6 mm. Always a particular "eye" of the stereo camera was used and portions of a track near to "holes" of local

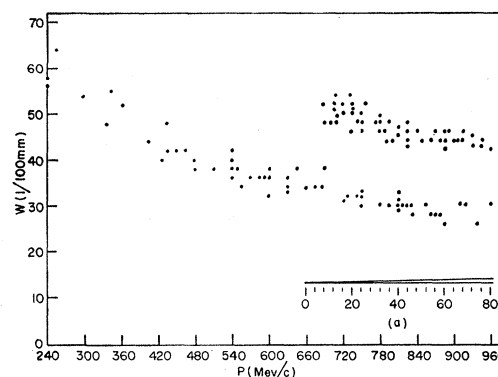


FIG. 3. Apparent track widths  $W$  measured at the projector by device sketched at (a), vs momentum  $P$ .

vapor depletion were avoided. When widths measured in this way are plotted against momentum, the points fall into separate groups as shown in Fig. 3. The identification of events in the deuteron group was checked in every case by comparing the track in question with protons nearby in the same picture. This check is easiest if there are present protons of the same momentum as the deuteron (and 40 percent the ionization) and protons of half the momentum (and the same ionization); however protons between these particular limits of momentum are always present and can also serve as checks. Such protons ionize less than a deuteron although they have less momentum. Figure 4 shows a deuteron (a) of momentum 1010 Mev/ $c$  (250 Mev), a proton (b) of the same momentum (437 Mev), and a proton (c) of half the momentum (127 Mev). It is seen that in ionization (a) and (c) are similar and noticeably exceed (b).

The deuteron group includes several tracks accompanied by electron pairs, resulting from internal conversion of a neutral pion gamma ray. These cases are identifiable as deuterons by kinematical arguments alone, without resort to ionization.

The validity of width measurements made in this way was verified separately by measuring track widths on the film with a recording microdensitometer. Every second deuteron was so measured, and also a comparable number of protons of various momenta, making a total of about 100. In Fig. 5 a typical microdensitometer trace is shown, and the width is defined as illustrated there. Widths measured in this way were consistently proportional to widths measured at the projector by the method described above and when plotted against momentum gave two adequately separated groups of points, as shown in Fig. 5. The microdensitometer used here is not a means of scanning, but rather an objective verification of the measuring technique used in scanning.

The relation between track width on the film and particle momentum depends on many factors, some of which are sketched here for the purpose of showing that in this experiment the width was mainly of optical

<sup>7</sup> R. H. Frost and C. E. Nielsen, Phys. Rev. **91**, 864 (1953).

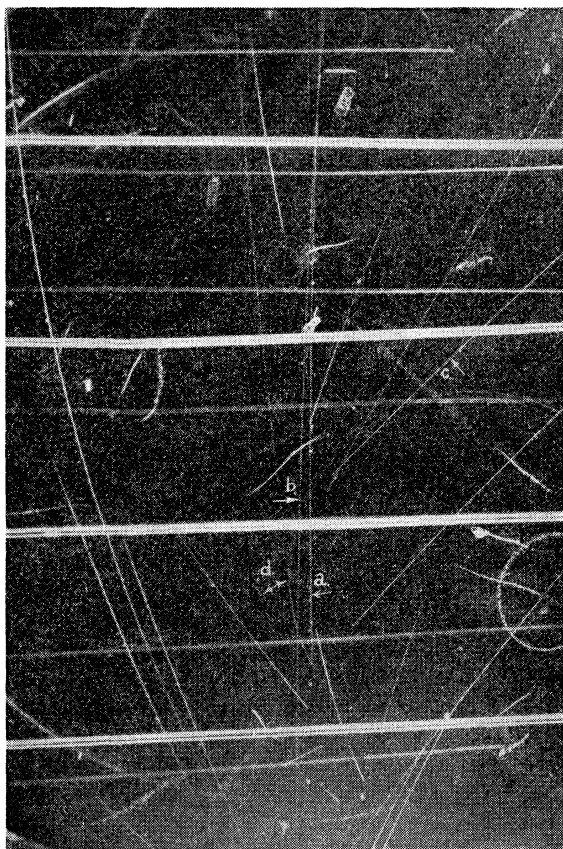


FIG. 4. Cloud-chamber picture showing deuteron (a), proton (b) of same momentum as deuteron, proton (c) of half that momentum, and electron pair (d) from internally converted neutral pion.

origin. At other than extreme relativistic energies the initial column of ions is effectively a line, except for recognizable delta rays. After formation, the ions diffuse at a rate depending on droplet size, which depends in turn on the rate of droplet growth, and therefore on the local density of vapor within the track volume and the rate of inward diffusion of vapor. For the cloud chamber used in this experiment the radius to which droplets have diffused at the time of photography is of the order of a few hundredths of a millimeter, a distance considerably smaller than the measured track half-widths. The increase in width is due to optical aberrations and film turbidity and granularity. This point was checked by photographing under typical conditions a very fine wire; the photographic image width was found to vary with about the 0.4 power of the illumination in the region of widths of interest in this experiment. Since the width is observed to vary with about the 0.2 power of the rate of ionization, the light scattered must vary approximately as the square root of the ionization, showing that droplet size does indeed depend on the density of ionization.

It is clear that obtaining consistent results in measuring ionization demands that tracks be formed in regions of the same supersaturation, that illumination be uniform, that the scattering angle of light into the camera be the same, that the optical settings of the camera be constant, and that the film be developed uniformly. In this experiment the first three conditions were approximated by using a well-collimated neutron beam thereby confining events to a nearly constant height and distance from the light source. Furthermore, the rather long interval of 27 seconds between pictures allowed full recovery of the chamber and lessened fluctuations of vapor density, as did the precautions to lessen unwanted background described in Sec. II.

### V. MEASUREMENT OF DEUTERONS

A chamber picture is conveniently divided into 7 sections by the images of the clearing grid wires, which are at right angles to the neutron beam. In order to have sufficient track length for accurate momentum measurement only deuterons originating in sections 2, 3, and 4 (the part of the chamber nearest the entrance window) were recorded. As a check on scanning efficiency, 1400 pictures containing 29 deuterons were carefully scanned a second time, and no additional deuterons were discovered.

Each deuteron was found to satisfy the kinematical relations displayed in Fig. 6, where  $P_d$  and  $\psi_d$  are the laboratory momentum and angle of the deuteron.<sup>8</sup> For each incident neutron energy  $T_n$  the possible deuteron angles and momenta in the laboratory lie on a curve on which the center-of-mass angle  $\psi_\pi$  of neutral pion emission can be marked off as a parameter. In general a given laboratory system angle and momentum for the deuteron correspond to a particular incident neutron energy and center-of-mass angle of pion emission. How-

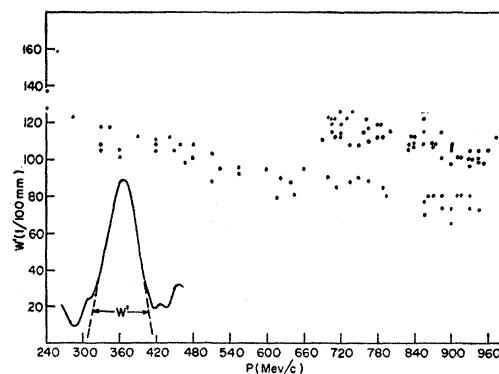


FIG. 5. Track widths  $W'$ , measured by means of recording microdensitometer, vs momentum. A typical densitometer trace is shown with the width  $W'$  defined.

<sup>8</sup> Deuterons could conceivably be produced in radiative capture of neutrons by protons. The cross section for radiative capture at 400 Mev is estimated by detail balance from the inverse reaction, high-energy photodisintegration of the deuteron, to be about  $10^{-20}$  cm<sup>2</sup>. The probability that one such event occurred in this experiment is about 1/10.

ever in the region of  $\bar{\psi}_\pi = 30^\circ$  to  $80^\circ$  curves for various  $T_n$  overlap, and  $T_n$  cannot be determined. Also the pion angle is not determined as sharply in this region. For these reasons, the center-of-mass angular distribution of pions and the excitation function for the reaction were found using only pion angles of  $90^\circ$  to  $180^\circ$ , where energy and angular resolution is good.

Each event was plotted on a graph like Fig. 6, and the meson angle and incident neutron energy read off. The intervals of error are shown by the rectangle in Fig. 6.

A total of 102 deuterons have been plotted in the angular distribution, 74 from runs with neutrons produced by a beryllium target and for which the neutron flux and spectrum have been measured as described in Sec. VI, and 28 from a shorter run with similar experimental arrangement, except that a deuterated paraffin target was used for neutron production.

Of the 102, 50 involve meson production forward in the center-of-mass system and 52 backward. This is in satisfactory agreement with a distribution symmetric about  $90^\circ$  in the center-of-mass system.

These events in the backward hemisphere, the hemisphere in which angular and energy resolution is relatively good, are listed in Table II. Groups A and B are deuterons produced by neutrons made in a beryllium and a deuterated paraffin target, respectively.

The angular distribution in intervals of  $\mu = \cos \bar{\psi}_\pi$  is given in Table III. A normalized angular distribution of the form  $F(A, \mu) = (A + \mu^2)/(A + \frac{1}{3})$  was fitted to these points by the statistically efficient maximum likelihood

TABLE II. Compilation of neutral pion production events used in determining angular distribution. The quantity  $T_n$  is the incident neutron energy and  $\bar{\psi}_\pi$  the center-of-mass pion angle for each event.

A				B			
$T_n$	$\bar{\psi}_\pi$	$T_n$	$\bar{\psi}_\pi$	$T_n$	$\bar{\psi}_\pi$	$T_n$	$\bar{\psi}_\pi$
440	31	390	2	415	17		
435	52	390	19	395	8		
435	68	390	33	395	18		
425	45	390	48	395	87		
425	81	390	78	390	18		
425	87	385	20	390	55		
420	8	385	27	385	39		
420	56	380	17	385	43		
415	51	380	50	380	51		
415	67	380	90	380	80		
405	30	375	41	370	49		
405	33	365	50	365	40		
405	62	365	60	365	68		
405	79	360	26	355	21		
400	42	355	80	350	38		
400	70	330	61	345	40		
395	33	320	70	340	9		
		315	41				

TABLE III. Number of events in intervals of  $\mu$ , the cosine of the center-of-mass pion angle.

$\mu$	1.0-0.8	0.8-0.6	0.6-0.4	0.4-0.2	0.2-0	$\Sigma=52$
No.	18	16	5	7	6	

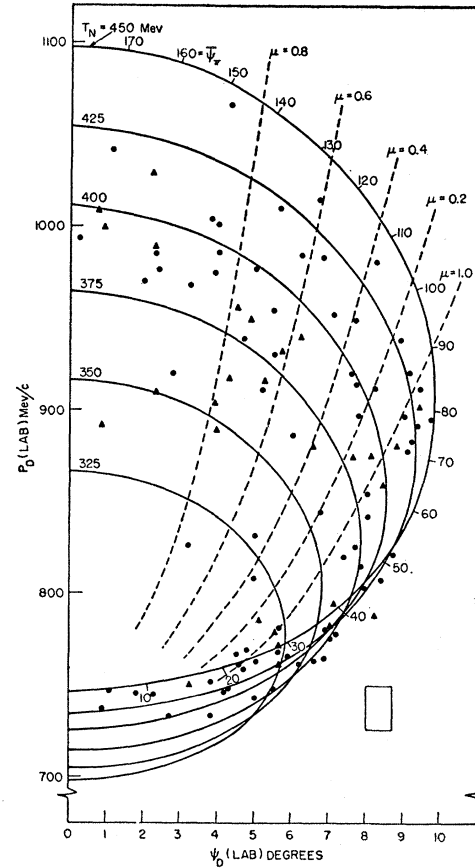


FIG. 6. Kinematics of pion-deuteron formation in  $n-p$  collisions. The term  $T_n$  is incident neutron energy,  $\psi_d$  and  $P_d$  are laboratory angle and momentum of the deuteron, respectively, and  $\bar{\psi}_\pi$  is the center-of-mass angle of pion emission. The dots represent events in run with beryllium target, the triangles events in run with deuterated paraffin target. The experimental error of these points is given by rectangle.

method.<sup>9</sup> Under the assumption that  $F(A, \mu)$  is an adequate theoretical description of the reaction, the likelihood that a given set of experimental points should have occurred is proportional to  $Q$ , where

$$Q = \prod_{i=1}^{52} F(A, \mu_i). \quad (2)$$

In Fig. 7  $Q$  is plotted as a function of the parameter  $A$  to be determined. The range of  $A$  containing 70 percent of the area under  $Q(A)$  is given by  $A = 0.28_{-0.14}^{+0.26}$ . The average energy of the neutrons making the pions in this angular distribution is 392 Mev, corresponding to a center-of-mass momentum and energy of the pion of 130 Mev/c and 53.3 Mev, respectively. Hildebrand<sup>2</sup> studied this reaction in the same beam using counter techniques and found  $A = 0.21 \pm 0.06$ . These limits are shown in Fig. 7.

<sup>9</sup> N. Arley and R. Buch, *Introduction to the Theory of Probability and Statistics* (John Wiley and Sons, Inc., New York, 1950), p. 142.

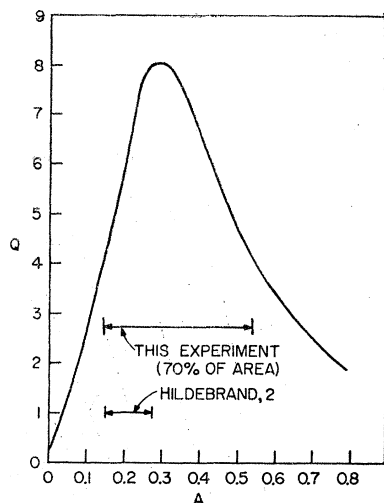


FIG. 7. Maximum likelihood function  $Q$  as a function of angular distribution parameter  $A$ .

Eight cases of internal conversion of a neutral pion were seen, four accompanied by deuterons and four by protons. The reactions are

- (A)  $n + p \rightarrow d + \pi^0 \rightarrow d + \text{pair} + \text{gamma ray}.$   
 (B)  $n + p \rightarrow n + p + \pi^0 \rightarrow n + p + \text{pair} + \text{gamma ray}.$

An example of reaction (A) is shown in Fig. 4, where (a) is the deuteron and (d) is the pair. The rate of internal conversion is presumably independent of the mode of creation of the neutral pion, since it lives long enough to escape its birthplace. The calculated<sup>10</sup> internal conversion coefficient is 0.0063 (per gamma ray) which agrees fairly well with the value  $0.0080 \pm 0.0016$  found in observations of neutral pions created in slow  $\pi^-$  capture by protons.<sup>11</sup> From the calculated rate of internal conversion one would expect one or two rather than four conversions in the 102 neutral pions studied in this experiment; in fact the probability that four or more conversions should occur is about 5 percent.

The four cases of reaction (B) give a crude estimate of the rate of neutral pion creation with unbound final nucleons. Using the theoretical internal conversion coefficient, one would expect these four cases to be accompanied by about 300 unconverted pions with unbound final nucleons, compared to 102 pions with bound final nucleons. The unbound reaction appears to be favored by a factor of the order of 3.

It has been pointed out by Serber<sup>12</sup> that deuterons produced in the reaction  $p + p \rightarrow d + \pi^+$  should be polarized. Such polarization present in the reaction studied in this experiment might be detected by scattering of the deuterons in the hydrogen of the chamber. No such

scatterings were observed. If the cross section is geometrical, the probability of such a scattering in this experiment is  $\frac{1}{5}$ . The scattering of polarized deuterons by larger nuclei may show asymmetry, in which case the insertion of a plate into the chamber might yield enough scatterings to permit study of the polarization. Such a plate should have low thermal conductivity in order to minimize its effect on chamber operation.

## VI. INCIDENT NEUTRON BEAM MEASUREMENTS

A sufficient number of neutron recoil protons were measured to (1) make statistical errors due to their number small compared with that of the deuterons, (2) obtain the neutron energy spectrum, and (3) to measure the  $n-p$  angular distribution for small proton angles. That the latter should be in accord with published data on the  $n-p$  angular distribution is a check on scanning methods.

While deuterons were measured, as mentioned, in regions 2, 3, and 4 of the chamber, protons were measured in region 3 only. This procedure gave about 9 protons measured per deuteron. Scanning criteria were: radius of curvature 210 cm or greater (momentum  $\geq 700$  Mev/c, energy  $\geq 235$  Mev) and the angles of the projector table (Fig. 2)  $\phi$  and  $\theta$  each less than  $30^\circ$ . Protons from the reaction  $n + p \rightarrow n + p + \pi^0$ , mentioned in Sec. V, very rarely have 235 Mev or more, so they introduce negligible error in the  $n-p$  scattering measurement. The time for measurement of one proton was 4-6 minutes. The relativistic center-of-mass angle of the proton and the laboratory energy of the incident neutron were determined by means of a computational routine requiring about  $1\frac{1}{2}$  minutes per event.

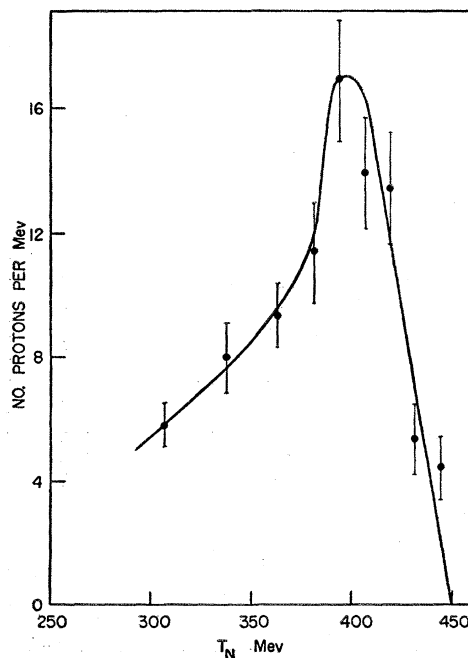


FIG. 8. Energy spectrum of incident neutron beam.

<sup>10</sup> R. H. Dalitz, Proc. Phys. Soc. (London) A64, 667 (1951).

<sup>11</sup> Lindenfeld, Sachs, and Steinberger, Phys. Rev. 89, 531 (1953).

<sup>12</sup> Cited in K. Watson and C. Richman, Phys. Rev. 83, 1256 (1951).

The neutron energy spectrum is shown in Fig. 8 and is derived from protons with center-of-mass angle less than  $45^\circ$ . The small variation of the total scattering cross section with energy has been taken into account. The energy resolution varies with the quality and length of the proton track; in most cases the energy half-width is about four percent. This spectrum is similar to the spectrum determined by Nedzel<sup>13</sup> using counter techniques in the same neutron beam.

In Fig. 9 the relative angular distribution for protons in the center-of-mass system is shown in integrated form. The ordinate gives the relative number of events with scattering angle cosine less than  $\mu$ . Only protons produced by neutrons of energy greater than 365 Mev are included, in order that the distribution can be compared with the results of Hartzler and Siegel<sup>14</sup> in a neutron beam with a very similar energy spectrum and using a detector with a threshold of about 365 Mev. Their results for the relative angular distribution have been converted to integrated form, normalized to ours by a multiplicative factor, and plotted as a line in Fig. 9. The agreement is satisfactory.

## VII. TOTAL DEUTERON CROSS SECTION

It is expected that the cross section for  $n+p \rightarrow d+\pi^0$  should have at these energies the approximate form:

$$\sigma = \alpha \eta^3, \quad (3)$$

where  $\eta$  = center-of-mass pion momentum in rest-mass units. The comparison of this equation with the em-

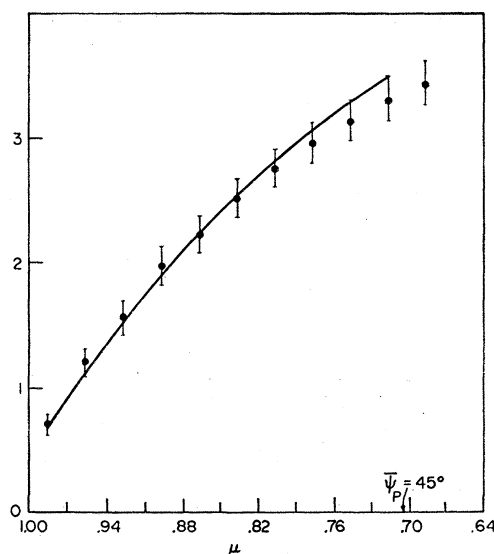


FIG. 9. Comparison of  $n-p$  scattering angular distribution obtained in this experiment (points with probable errors) with results of Hartzler and Siegel (reference 14) (line). The ordinate gives the relative number of events above a given value of  $\mu$ , where  $\mu$  is the cosine of the proton angle  $\psi_p$  in the center-of-mass system.

<sup>13</sup> V. A. Nedzel, Phys. Rev. **94**, 174 (1954).

<sup>14</sup> A. J. Hartzler and R. T. Siegel, Phys. Rev. **93**, 928 (1954) and **95**, 185 (1954).

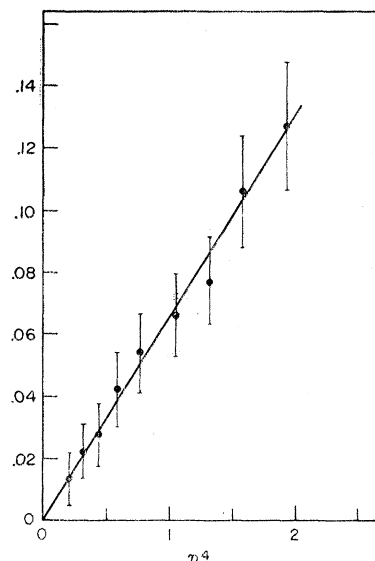


FIG. 10. Comparison of the empirical excitation function in  $n+p \rightarrow d+\pi^0$  with  $\eta^3$ . The results are plotted in integrated form and therefore are plotted against  $\eta^4$ . The ordinate represents  $\sum_{\eta_i \leq \eta} (n_{di}/n_{pi})$ .

pirical excitation determined from a small number of events is best done in the following way. Let  $n_{di}$  and  $n_{pi}$  be the numbers of deuterons and protons produced in some given interval of incident neutron energy. If the excitation follows Eq. (3), then the ratio  $n_{di}/n_{pi}$  is proportional to  $\eta_i^3$ , where  $\eta_i$  corresponds to the given energy interval and it is assumed that the  $n-p$  scattering cross section varies little over the energy range 300–450 Mev. The sum of the ratios up to some value of  $\eta$  will be proportional to  $\eta^4$ . In Fig. 10 this sum is plotted against  $\eta^4$  and the points are seen to be in reasonable agreement with a straight line, showing that the experimental variation of yield with energy is consistent with Eq. (3).

We now determine the constant  $\alpha$ . The number of  $n_{di}$  of deuterons produced by neutrons in the energy interval  $i$  is

$$n_{di} = \alpha \eta_i^3 L_i / C, \quad (4)$$

where  $L_i$  is the number of neutrons in energy interval  $i$  passing through the chamber and  $1/C$  is the number of scattering centers per  $\text{cm}^2$ . The number  $n_{pi}$  of protons produced with center-of-mass angle less than  $45^\circ$  by neutrons in the same energy interval  $i$  is

$$n_{pi} = (S\delta/K)(L_i/C), \quad (5)$$

where  $S$  is the total  $n-p$  scattering cross section and  $\delta$  is given by

$$\delta = \int_0^{45^\circ} \frac{d\sigma_{np}}{d\Omega} d\Omega / \int_0^\pi \frac{d\sigma_{np}}{d\Omega} d\Omega. \quad (6)$$

The factor  $K=2.84$  accounts for the fact that a larger section of each picture was scanned for deuterons than



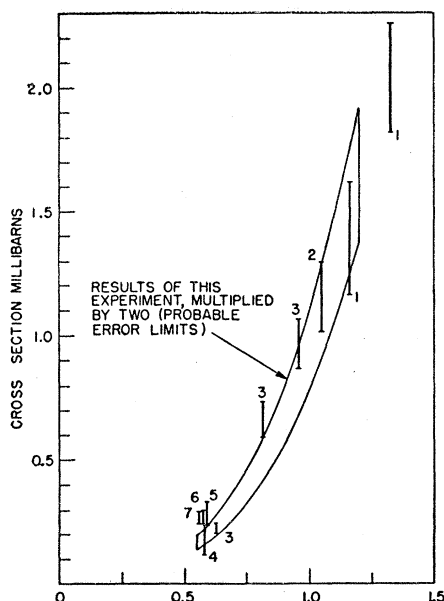


FIG. 11. Comparison of two times the total cross section for  $n+p \rightarrow d+\pi^0$  with the total cross section for  $p+p \rightarrow d+\pi^+$ , as a test of charge independence. Points are: 1, Stadler (reference 15); 2, Fields *et al.* (reference 17); 3, Durbin *et al.* (reference 3); 4, Cartwright *et al.* (reference 18); 5, Clark *et al.* (reference 16); 6, Crawford and Stevenson (reference 20); 7, Schulz (reference 19) normalized by Rosenfeld (reference 1) to Crawford and Stevenson (reference 20).

for protons. The total number of deuterons  $N_d$  is given by

$$N_d = \frac{\alpha}{S\delta} K \sum_i \eta_i^3 n_{pi}, \quad (7)$$

where it is assumed that  $\delta$  and  $S$  are not strongly varying with energy. This experiment, then, determines directly  $\alpha/S\delta$  to be  $0.058 \pm 0.0088$ .

From the result of Hartzler and Siegel<sup>14</sup> the factor  $\delta$  is found to be  $0.240 \pm 0.010$ . The error given is determined by first maximizing and then by minimizing  $\delta$  within the probable errors of Hartzler and Siegel's points.

The total  $n-p$  scattering cross section  $S$  has been measured by Nedzel<sup>13</sup> in the same neutron beam used in this experiment and is  $33.7 \pm 1.3$  mb. Combining  $S$  and  $\delta$  with our result, we find

$$\sigma(n+p \rightarrow d+\pi^0) = (0.47 \pm 0.08) \eta^3 \text{ millibarns}. \quad (8)$$

At 392 Mev, the mean incident energy of events in this experiment, the cross section is  $0.41 \pm 0.07$  mb. The comparison of Eq. (8) with data on the reaction  $p+p \rightarrow$

$d+\pi^+$  is made in Fig. 11, in which twice Eq. (8) is plotted in order that Eq. (1) may be checked directly. The charged pion production results plotted in Fig. 11 come from the inverse reaction measured by Stadler,<sup>15</sup> by Durbin *et al.*,<sup>3</sup> and by Clark *et al.*,<sup>16</sup> and from the direct pion production reaction measured by Field *et al.*,<sup>17</sup> Cartwright *et al.*,<sup>18</sup> by Schulz,<sup>19</sup> and by Crawford *et al.*<sup>20</sup> The agreement, within the errors of the experiments, is a confirmation of Eq. (1) predicted by charge independence.

## VIII. CONCLUSION

With regard to experimental methods, the operation of a high-pressure hydrogen diffusion cloud chamber under conditions such that the angle, momentum and ionization of positive recoils could be measured has been described. The conditions permitting consistent ionization measurement have been discussed.

With regard to the reaction  $n+p \rightarrow d+\pi^0$  studied here, it was found that the total cross section agrees within the accuracy of the experiment with the prediction of charge independence in the pion-nucleon interaction. The angular distribution found agrees with the previous measurement<sup>2</sup> made by an entirely different method. Cases of internal conversion of the neutral pion give evidence that neutral pion production with unbound final nucleons occurs at a rate comparable to that for production with bound final nucleons.

The author is grateful for the pleasure of association with Dr. S. C. Wright during the development and use of the cloud-chamber system. The skill of Mr. R. Barrons of the Physical Sciences Development Shop was invaluable throughout this work. The cyclotron operating crew directed by Mr. Lester Kornblith, Jr., was most cooperative. The assistance of Mr. Lawrence Rosenson, particularly in scanning, is gratefully acknowledged. Grateful acknowledgment is made to the U. S. Atomic Energy Commission and to the Eastman Kodak Company for fellowship appointments during this project. The author is most indebted to Professor Enrico Fermi for his constant guidance and encouragement throughout this research.

<sup>15</sup> H. Stadler (private communication).

<sup>16</sup> Clark, Roberts, and Wilson, Phys. Rev. **83**, 649 (1951).

<sup>17</sup> Fields, Fox, Kane, Stallwood, and Sutton [Phys. Rev. **95**, 638 (1954)] total cross section amended slightly in report to the 1954 Washington meeting.

<sup>18</sup> Cartwright, Richman, Whitehead, and Wilcox, Phys. Rev. **91**, 677 (1953).

<sup>19</sup> A. G. Schulz, Jr., University of California Radiation Laboratory Report UCRL-1756, 1952 (unpublished).

<sup>20</sup> F. S. Crawford, Jr., and M. L. Stevenson, Phys. Rev. **91**, 468 (A) (1953).

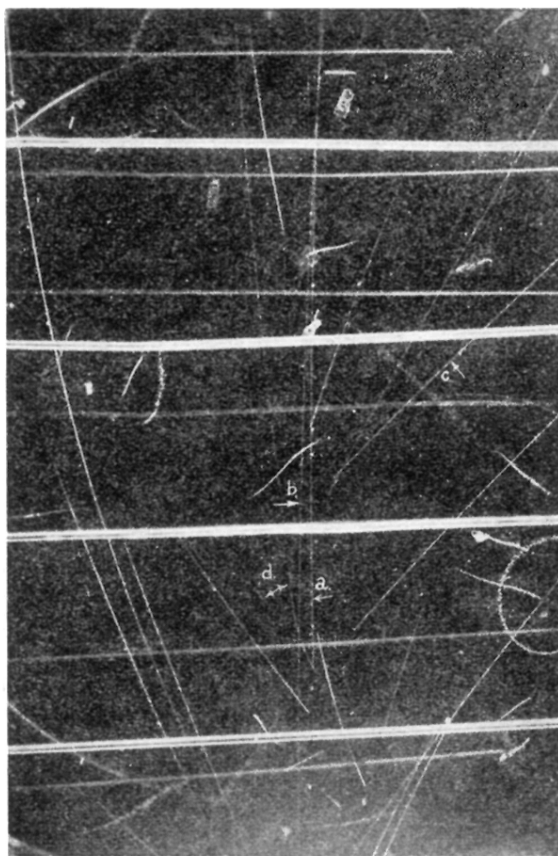


FIG. 4. Cloud-chamber picture showing deuteron (a), proton (b) of same momentum as deuteron, proton (c) of half that momentum, and electron pair (d) from internally converted neutral pion.